

Accurate 3D Localization for 60 GHz Networks

Ioannis Pefkianakis

Hewlett Packard Labs

Palo Alto, California

ioannis.pefkianakis@hpe.com

Kyu-Han Kim

Hewlett Packard Labs

Palo Alto, California

kyu-han.kim@hpe.com

ABSTRACT

RF-based (mainly Wi-Fi and BLE) localization systems have been gaining the significant amount of attention from industry, since they do not require the deployment of any special and costly infrastructure such as cameras and depth sensors but leverage existing wireless Access Points (APs) and mobile clients. However, extensive field trials have shown that such solutions can be *inaccurate* (e.g., meter-level localization error) and/or *impractical* (e.g., requiring centrally-controlled, dense AP deployments). In this paper, we focus on millimeter-wave wireless networks, which are becoming increasingly popular for both indoors and outdoors connectivity, to overcome the aforementioned limitations and to provide accurate 3D localization. Specifically, we propose *mWaveLoc*, a system that exploits the small wavelength (millimeter) and directional communication of millimeter-wave (e.g., in 60 GHz) networks for accurate and practical 3D localization. *mWaveLoc* relies only on a single AP to track a device's position and works with existing off-the-shelf 802.11ad 60 GHz devices. Our implementation and experimental results on commodity 802.11ad testbeds show that *mWaveLoc* can achieve centimeter-level AP-client distance estimation accuracy and decimeter-level 3D localization accuracy in Line-Of-Sight settings.

CCS CONCEPTS

• Networks → Location based services;

KEYWORDS

Millimeter-Wave, 60 GHz, 802.11ad, Localization

ACM Reference Format:

Ioannis Pefkianakis and Kyu-Han Kim. 2018. Accurate 3D Localization for 60 GHz Networks. In *SenSys '18: Conference on Embedded Networked Sensor Systems, November 4–7, 2018, Shenzhen, China*. ACM, New York, NY, USA, 12 pages. <https://doi.org/10.1145/3274783.3274852>

1 INTRODUCTION

Wireless RF-based device localization and tracking¹ have been attracting significant attention from industry [10, 13, 19, 50], as a key enabler of a wide range of applications, such as: (a) navigation in

¹In this paper we use the terms, “positioning”, “tracking”, and “localization”, interchangeably.

Permission to make digital or hard copies of all or part of this work for personal or classroom use is granted without fee provided that copies are not made or distributed for profit or commercial advantage and that copies bear this notice and the full citation on the first page. Copyrights for components of this work owned by others than ACM must be honored. Abstracting with credit is permitted. To copy otherwise, or republish, to post on servers or to redistribute to lists, requires prior specific permission and/or a fee. Request permissions from permissions@acm.org.

SenSys '18, November 4–7, 2018, Shenzhen, China

© 2018 Association for Computing Machinery.

ACM ISBN 978-1-4503-5952-8/18/11.

<https://doi.org/10.1145/3274783.3274852>

large buildings, campuses or stadiums [50], (b) device-to-device localization to connect people in physical proximity, (c) occupancy sensing [36], (d) virtual and augmented reality [22, 37], and (e) vehicle positioning [57]. The key advantage of RF-based localization and tracking systems is that they do not require the deployment of special and/or costly infrastructure, such as cameras and depth sensors [4, 34], and they can simply rely on existing wireless Access Points (APs) and mobile clients. Moreover, different from acoustic-based [21, 43] or visible light-based [11, 49] localization, RF-based localization and tracking does not typically require Line-Of-Sight (LOS) communication between AP and client devices, yet cover longer ranges.

However, despite such a wide adoption, extensive field trials have shown that such solutions still suffer from high error and practical challenges. Specifically, recent studies and industry deployments [13, 17, 19, 50] reveal that a location estimation error can be in the order of several meters in realistic indoor scenarios. Moreover, such systems often require dense infrastructure (Wi-Fi AP or BLE beacon) deployment, and APs should operate on the same channel or need special antenna technology [13]. These requirements impose high overheads in the network, thus limiting their practicality.

Recently, millimeter-wave (mmWave) wireless networks become de facto a key enabling technology for 5G mobile broadband [1–3] and gigabit-speed WLAN or wireless backhaul connectivity [20, 44, 58], and further, they open new horizons for device localization and tracking. Due to their high operational frequency (*i.e.* 60 GHz for 802.11ad networks [29]) and their short wavelength (*i.e.* 5mm for 802.11ad networks), mmWave wireless signals can help track a device's position at a very fine (millimeter-level) resolution [54]. However, in spite of the promise, state-of-art mmWave tracking solutions are still in their infancy in terms of adoption and deployment for several reasons. First, they often require specialized hardware [6], *a priori* knowledge of physical environment [7] and multiple APs [24, 54] to estimate a device's position. Next, their performance has been mainly evaluated through SDRs (Software Defined Radios) with horn antennas or simulations, without considering the limitations of commodity mmWave hardware.

In this work, we present *mWaveLoc*, a *high-accuracy 3D localization system, for commodity 802.11ad 60 GHz mmWave networks*. *mWaveLoc* leverages the existing 802.11ad network infrastructure, which becomes increasingly popular for both indoors [44, 55, 58] and outdoors [20] connectivity. While *mWaveLoc* focuses mainly on indoor applications mentioned above, it can be used for outdoor applications such as vehicle positioning. In its core, *mWaveLoc* seeks to overcome the limitations of existing systems by setting the following design goals:

Decimeter-level 3D localization: *mWaveLoc* aims to improve localization accuracy of existing deployed RF-based systems from

meter-level to decimeter-level. Further, different from existing Wi-Fi systems that support 2D space localization, *mWaveLoc* can track a device on 3D space enabling new applications such as position-dependent VR/AR [22, 37] and mobile robot navigation [34].

Single-AP localization: While existing systems require centrally-controlled and dense wireless infrastructure, *mWaveLoc* relies only on two connected devices (*e.g.* an 802.11ad AP and client) for localization. This allows for low-latency tracking that is critical for VR/AR applications as well as for device-to-device location applications.

Robust localization: *mWaveLoc* seeks to provide accurate localization under device mobility or environmental blockages, even with challenging 60 GHz operational link. In contrast to existing work that focuses on short range (3-4 m) tracking (*e.g.* [37]), *mWaveLoc* supports longer range (> 20m) localization.

Practical localization: *mWaveLoc* needs to be an 802.11-compliant, lightweight system that can be implemented in 802.11ad off-the-shelf devices without requiring any specialized, expensive hardware. It should be fully implementable at the AP side, without requiring any changes in client devices.

mWaveLoc achieves these goals by leveraging two key properties of 802.11ad 60 GHz networks as follow:

Directional communication: mmWave devices use phased-array antennas to focus their RF energy through directional beams (*i.e.* beamforming), compensating the attenuation loss at very high frequency (60 GHz) bands. Intuitively, the best (highest signal strength) beams are the ones that are aligned with the azimuth and elevation direction of the LOS wireless propagation path between the transmitter and receiver. Thus-identified (best) beams can help find the direction of the LOS path and the position of the device.

Short wavelength communication: The distance estimation granularity between two devices is proportional to the carrier frequency and hence to the wavelength. Operating on 60 GHz (5mm wavelength), 802.11ad devices can yield high granularity and achieve high distance estimation accuracy.

In a nutshell, *mWaveLoc* leverages CIR (Channel Impulse Response) measurements to identify the wireless 60 GHz multipath environment between two 802.11ad devices. Specifically, upon collecting and sanitizing CIR measurements from the directional beams available in 802.11ad platform, *mWaveLoc* first extracts the LOS path for each beam, excluding Non-LOS (NLOS) paths from strong reflectors. Next, *mWaveLoc* selects a constant number of beams that amplify the most the LOS path, and correlates the beam amplitudes with the beam patterns (known *a-priori* at the 802.11ad device), to identify an area where the azimuth and elevation direction of the LOS path (and hence the mobile device) lies with high probability. Finally, using a simple geometric model, it identifies the mobile device's angular position. Our evaluation results show that *mWaveLoc*'s angular position estimation is highly accurate, despite the "imperfect" beams (with strong side lobes) in commodity 802.11ad devices.

mWaveLoc further leverages an 802.11-compliant Fine Timing Measurement (FTM) scheme to accurately measure the Time of Flight - ToF - *i.e.* the round trip propagation time of a signal transmitted between two devices. Upon appropriately calibrating the ToF measurements, *mWaveLoc* estimates the distance between the devices. Different from existing work [54] that estimates distance

via erroneous phase shift tracking, *mWaveLoc* remains robust to phase-incoherences observed in commodity 802.11ad platforms.

We have implemented *mWaveLoc* in the kernel of a commodity 802.11ad AP platform, without modifying any 802.11ad core functions (*e.g.* beam selection, codebook design etc.). We have extensively evaluated our implementation in multiple static and pedestrian mobility scenarios, with both open LOS communication and blockages, in various AP-client distances, ranging from 0.25 to 22 meters. As ground truth, we use the 3D location estimated by an infrared light HTC Vive base station and controller [52]. Our extensive evaluation results show that, *mWaveLoc* achieves *decimeter-level 3D localization accuracy* (*i.e.* < 1 meter estimation error) in approximately 73% of our evaluated settings, with median estimation error to be 75 cm. Even under blockages, AP-client antenna misalignments and long AP-client separation distances, *mWaveLoc* achieves decimeter-level 3D localization accuracy in the majority of the cases, as soon as there is a LOS path between AP and client devices. When the LOS path is persistently, fully blocked (*e.g.* under human blockage), *mWaveLoc*'s location estimation error can be in the order of meters. We consider such scenarios to be infrequent in very dense 60 GHz AP deployments [55]. Finally, *mWaveLoc*'s FTM scheme can achieve *centimeter-level distance estimation accuracy* in LOS, with median estimation error to be 4 cm. On the other hand, existing approaches (such as non-coherent path tracking [14, 39]) have a median and maximum estimation error of 2.7 and 10.3 meters, respectively. *To our best knowledge, mWaveLoc is the first implementation and evaluation of 3D localization using commodity 802.11ad devices.*

The rest of the paper is organized as follows. In Section 2, we present a critique of related designs, using data collected from our 802.11ad platform. In Section 3, we present *mWaveLoc*, a high-accuracy 3D localization system, for commodity 802.11ad 60 GHz networks. Finally, in Sections 4 and 5, we explain the implementation and evaluation of *mWaveLoc*, with off-the-shelf commodity 60GHz testbeds.

2 RELATED WORK

There is a vast amount of literature on wireless indoor localization [23]. However, the solutions deployed in large buildings (*e.g.* enterprise and campus settings) are typically Wi-Fi [13, 16, 38, 50] or BLE-based [10, 19] localization systems. Recent Wi-Fi localization proposals claim decimeter [16, 38] or even centimeter [37] level accuracy, for short-range, small AP-client topologies. However, field trials and industry deployments [13, 17, 50] have shown that WiFi-based localization can be *inaccurate*, resulting in several meters error. BLE localization suffers from several meters error as well [19]. Moreover, such systems are often *impractical* requiring (*a*) dense AP (or BLE beacon) deployment where APs operate on the same channel, (*b*) special antenna technology, (*c*) high probing overheads, and (*d*) are affected by hardware noises and clients' configurations. On the other hand, mmWave networks hold great potential to achieve higher accurate localization by operating on shorter (millimeter) wavelengths.

Next, we discuss the design of existing mmWave localization systems and their limitations in three categories:

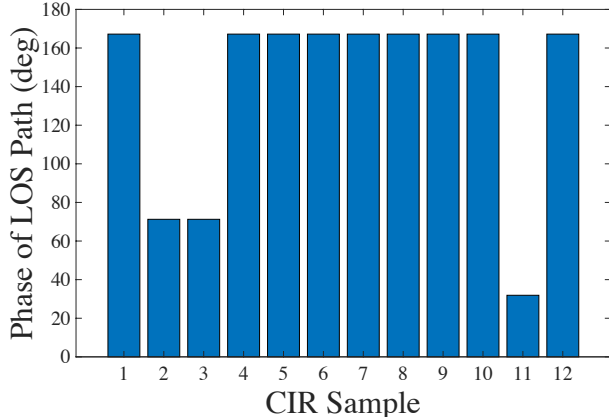


Figure 1: Phase variation of the LOS path between a static 802.11ad AP and client, measured using commodity 802.11ad devices.

MIMO-based mmWave localization: Recent research proposals [9, 26, 28] introduce user localization algorithms for MIMO mmWave wireless networks. Such algorithms estimate signal Angle-of-Arrival (AoA) using angular spectrum analysis, assuming that mmWave devices are equipped with digital phased arrays. For example, authors in [26] apply MUSIC [46] to estimate AoA, in 60 GHz settings. However, such approaches are not applicable to 802.11ad devices, because they are not MIMO-capable and only support analog phased arrays. E-Mi [53] proposes to emulate a digital phased array. It samples the same signal using different weights (*i.e.* codebook) at an analog phased array receiver, isolates the signals on each antenna element, and applies MUSIC [46] to estimate the AoA, AoD (Angle-of-Departure) of each mmWave propagation path. However, in practice, the weight vectors of 802.11ad phased arrays are pre-defined and built into hardware, and further they change only if the current beam performs poorly. Different from such approaches, our proposed *mWaveLoc* does not require MIMO or any firmware modifications, but works with off-the-shelf 802.11ad devices.

Phase tracking-based mmWave localization: mTrack [54] was proposed to track passive objects at sub-centimeter precision. It leverages a discrete mmWave beam scanning scheme to pinpoint the object’s initial location, and tracks its trajectory by tracking the signal phase shifts. However, channel measurements from off-the-shelf mmWave platforms are phase-incoherent [31, 39], due to the lack of carrier phase tracking across different packets. For example, Figure 1 shows the phase of the LOS path measured with our 802.11ad AP and client, for 12 consecutive Channel Impulse Response (CIR) samples, in a fully controlled, static setting. We observe phase shifts up to 136°, even without mobility.

Sector-sweep-based localization: Designs such as PLAT [33], correlate measurements (*e.g.* ToF, SNR, angular offsets) from multiple narrow beams to identify the orientation of the LOS (and NLOS) paths, and hence locate the client. Although PLAT is a single-AP, single-RF chain localization scheme, it can be impractical for three reasons. First, it requires a dedicated sector-level sweep scheme for localization (other than the 802.11ad SLS/BRP) and per-beam ToF estimation, whose overhead is prohibitive, especially when an AP

serves very low latency applications. Second, PLAT is not 802.11 standard compliant since it requires specific AP-client collaboration. Finally, it assumes narrow beams, which may not be supported in commodity systems (*c.f.* Section 3.1). Similar to PLAT, non-coherent path tracking approaches [14, 39] estimate the azimuth and elevation of the LOS path between a transmitter-receiver pair (and hence receiver’s location), by correlating the radiation patterns with the SNRs of a selected set of beams. Our results presented in Section 5 show that such approach is highly inaccurate, due to the imperfect beam patterns used by commodity 802.11ad devices.

Other limitations: Existing mmWave device tracking approaches may require; (*a*) multiple network interfaces (*e.g.* Wi-Fi and 60 GHz [44, 56]), (*b*) specialized hardware (*e.g.* fine-grained phase array control [6]), (*c*) a-priori knowledge of the physical environment [7] (*e.g.* room geometry), or (*d*) dense infrastructure (*e.g.* 1 transmitter and 2 receivers in [54], multiple 802.11ad APs in [24]) or multiple anchor points [27, 32], which limit their practicality in realistic settings. Our proposed *mWaveLoc* system does not have any of the above requirements. Moreover, different from most of the existing mmWave designs which have been evaluated with SDRs, horn antennas or simulations, we evaluate *mWaveLoc* in commodity 802.11ad testbeds.

3 DESIGN

This section presents the design of *mWaveLoc*, a high-accuracy 3D localization system, for commodity 802.11ad 60 GHz mmWave networks. *mWaveLoc* sets two key design goals – *high accuracy* and *practicality*.

High accuracy: *mWaveLoc* aims to achieve decimeter-level 3D localization accuracy using commodity 802.11ad hardware, which is adequate to accommodate popular location-based applications. In Section 5, we show that *mWaveLoc* can achieve this goal as soon as there is a LOS path between the AP and client devices.

Practicality: *mWaveLoc*’s goal is to provide accurate localization between two communicating 802.11ad devices (*e.g.* one AP and client), without requiring centrally-controlled and dense wireless infrastructure. Single-AP localization can allow for low-latency tracking, which is critical for 3D VR/AR applications. *mWaveLoc* needs to be an 802.11-compliant, lightweight system that can be implemented in 802.11ad off-the-shelf devices, without requiring any specialized, expensive hardware. It should not require any modifications in existing 802.11ad core functions (*e.g.* beam selection, codebook design, etc.). It should be fully implementable at the AP side, with no client-side support.

Intuition: An *mWaveLoc* AP could accurately localize a client by identifying the length d , and the azimuth and elevation directions (θ^{az}, θ^{el}) of the Line-Of-Sight (LOS) wireless propagation path between the two devices, denoted as P_1 in Figure 4(a)². *mWaveLoc* leverages CIR (Channel Impulse Response) measurements from a constant number of beams and correlates the measurements with the beam patterns known *a-priori* at the AP, to track the angular position of the client device. Then, it employs a Fine Timing Measurement (FTM) scheme to precisely estimate the AP-client distance.

²LOS path signal is the signal component that traverses along the straight line joining the 802.11ad AP and client.

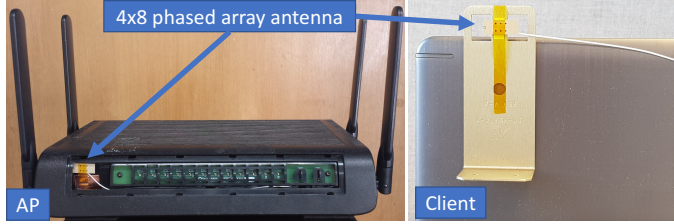


Figure 2: Our 60 GHz 802.11ad AP and client devices, which use 4×8 phased arrays.

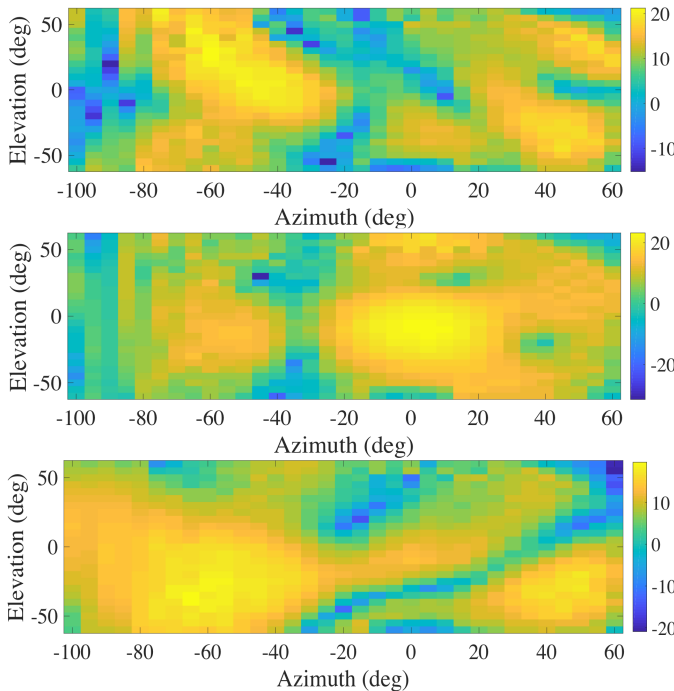


Figure 3: Radiation patterns of three different beams in our platform. Signal strength is in dB.

We next discuss 802.11ad background related to our intuition, and then elaborate our design.

3.1 A Primer on 802.11ad Beamforming

The focus of this paper is on 802.11ad [29] devices, which operate on the 60 GHz unlicensed spectrum. 802.11ad devices support 2.16 GHz channel bandwidths and PHY rates up to 7 Gbps. 802.11ad can overcome high-frequency propagation loss at 60 GHz, by using phased array antennas to steer RF energy towards narrow spatial directions/beams (*i.e.*, beamforming) [25, 41]. For a 1D linear phased-array antenna, the gain of the m^{th} beam pattern can be expressed as [35]:

$$A_m(\theta) = \sum_{n=1}^N \mathbf{w}(n, m) \cdot e^{(j2\pi n d \cos\theta / \lambda)} \quad (1)$$

where N is the number of antenna elements (with uniform separation d) and λ is the wavelength of the wireless signal. The weights $\mathbf{w}(n, m)$ can be tuned to generate different beams with diverse radiation patterns. Commodity 802.11ad devices typically use 2D phased

array antennas and can generate radiation patterns in both azimuth and elevation directions denoted by $A_m(\theta^{az}, \theta^{el})$. For example, Figure 2 shows the 4×8 2D phased-array antenna of our 802.11ad testbed's AP and client devices. Figure 3 further shows the azimuth and elevation radiation patterns of three example beams of our 802.11ad AP platform. Notice that the beam patterns are far from a perfect shape, due to discrete configuration weights [31, 35, 39, 44]. Finally, all the beam patterns A_m are predefined, built into hardware, and are known *a priori*.

IEEE 802.11ad specifies a beamforming training (BFT) process to discover the highest signal strength transmit (Tx) and receive (Rx) beams between a pair of devices. BFT comprises of a mandatory Sector Level Sweep (SLS) phase and an optional Beam Refinement Phase (BRP). SLS and BRP hierarchically evaluate the Tx and Rx beam combinations to identify the best one [29, 45]. During SLS and BRP beam scanning, the initiating device (*e.g.* AP) collects channel (CIR) feedback for each available beam. We next show how *mWaveLoc* leverages 802.11ad beamforming for angular position tracking.

3.2 Tracking Angular Position

mWaveLoc estimates the angular position of the client device with respect to the AP by leveraging two key properties of the 60 GHz wireless channel; channel sparsity and beam-independent path extraction.

Channel sparsity: In practice, mmWave channel is often sparse in that it contains only $1 \sim 3$ dominating wireless signal propagation paths [12, 40, 45, 48]. The number and the signal amplitude of each of these paths can be extracted by using PHY-layer information, called Channel Impulse Response (CIR) [51]. *mWaveLoc* uses CIR feedback to identify the LOS path and the beams that align the most with the path, as we discuss next.

Beam-independent path extraction: While changing beam patterns at a transmitter leads to different CIR measurements at a receiver, the underlying signal paths traversed by each of the beams remain the same. Typically, the beams that overlap the most with the signal propagation paths will show higher amplitude at the CIR measurements.

Based on the above properties, *mWaveLoc* can identify the mmWave multipath environment, and then, extract the LOS path between an AP and client. Specifically, by performing a complete beam scan, it can identify a subset of M beams that align the most with the LOS path. By correlating the LOS path amplitude of the selected M beams with their beam patterns, *mWaveLoc* can estimate client's angular position. In what is next, we will elaborate on these steps.

3.2.1 Identifying Multipath Environment. The mmWave signals from the AP to a mobile device arrive along S distinct paths, as shown in Figure 4 (for $S = 2$). Each path is described by its amplitude a_s , phase ϕ_s and azimuth, elevation directions $(\theta_s^{az}, \theta_s^{el})$, where $s = 1, 2, \dots, S$. *mWaveLoc* needs to extract only the amplitude and angular information for the LOS path, described by the 3-tuple $(a_s, \theta_s^{az}, \theta_s^{el})$. To this end, it leverages the Channel Impulse Response (CIR) to measure the amplitude of the different wireless propagation paths (both direct and reflected). Since today's off-the-shelf 802.11ad devices allow 1.76 GHz channel measurement [29],

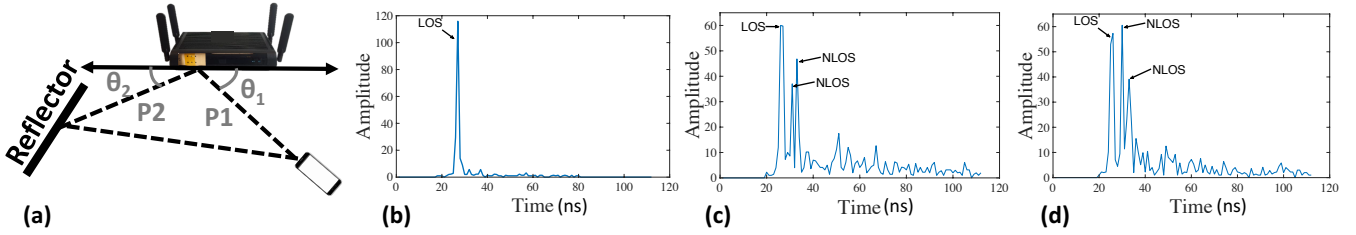


Figure 4: 60 GHz multipath environment measured with different beams: (a) Example of 60 GHz multipath environment, with two physical paths: P1 (LOS), P2 (NLOS). Paths can be captured by measured channel responses. (b–d) Measured channel responses show the arrival times of physical paths for beams 1 to 3. Notice that the measured amplitude of paths changes with the beam pattern.

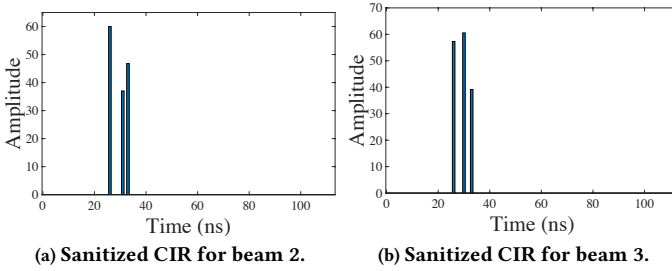


Figure 5: Wireless signal paths for beams 2, 3 (c.f. Fig. 4(c), 4(d)) after CIR sanitization. Each tap corresponds to one path.

mWaveLoc can measure each potential path with arrival time difference of 0.57 ns. For example, Figures 4(b–d) show the Power Delay Profile (*i.e.* amplitude of a signal received through a multipath channel as a function of time delay) based on collected CIRs in our AP platform. Now, *how can we extract the LOS path?*

CIR sanitization: Before proceeding to path extraction, *mWaveLoc* needs to separate the dominating paths' signals, from weak reflected signals or noises, which appear as low amplitude spikes in the Power Delay Profile. *mWaveLoc* isolates the dominating paths by identifying the local maxima, whose amplitude is not much smaller than the maximum amplitude path α_{peak} . Specifically, if $\alpha(t)$ is the amplitude at time t , our peak identification function is formally defined as:

$$\alpha(t) = \begin{cases} \alpha(t) & \text{if } \alpha(t) > \alpha(t-1) \text{ and} \\ & \alpha(t) > \alpha(t+1) \text{ and} \\ & \alpha(t) > \alpha_{peak}(t') - A_{tr} \\ 0 & \text{otherwise} \end{cases}$$

Here, A_{tr} defines the gap between the amplitude of the path $\alpha(t)$ compared to the peak amplitude path $\alpha_{peak}(t')$. Intuitively, A_{tr} should be set such that paths, whose distance from the peak is above A_{tr} , will not contribute to mmWave performance. Our extensive experiments show that setting A_{tr} to 5 dB satisfies the above requirement and always identifies the dominating paths. Figures 5a and 5b show the sanitized Power Delay Profile corresponding to the CIRs as presented in Figures 4(c) and 4(d), respectively. We

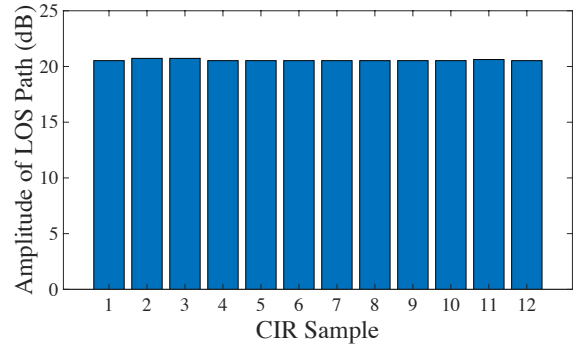


Figure 6: Amplitude deviation of the LOS path between a static 802.11ad AP and client, for back-to-back CIR samples.

observe that in both cases, our algorithm can successfully extract the 3 dominating paths.

LOS path extraction: The direct (LOS) path traverses the minimum distance among all the received paths, and it likely appears in the earliest component of the CIR. In Figures 4(b–d), the LOS path is the first spike in the Power Delay Profile. The reflected paths arrive with a delay at the receiver (*e.g.* in Figure 4(c) the 2nd and 3rd NLOS paths arrive with a delay of 2.85 and 3.99 ns, respectively). Notice that the LOS is not necessarily the highest amplitude path. Figure 4(d) shows that the beam 3 amplifies the reflected (NLOS) path more, resulting in the highest amplitude.

802.11ad hardware noises: As shown in Figure 1, phase can be incoherent between back to back samples in commodity 802.11ad devices. Fortunately, we found that such deviations are negligible if we consider the amplitude of back-to-back CIR samples. For example, Figure 6 shows the amplitude deviation (in dB) of the LOS path among back-to-back samples for the same scenario of Figure 1. We observe that amplitude standard deviation is negligible (only 0.08 dB), which makes our path extraction algorithm robust even under the 802.11ad hardware noises.

3.2.2 Angle Identification. Upon extracting the propagation paths, *mWaveLoc* seeks to identify the azimuth and elevation direction (θ^{az}, θ^{el}) of the LOS path that aligns with client's angular position. *mWaveLoc*'s angle identification algorithm is based on a simple intuition: *the LOS path will likely lay in the intersection of a set of M beams, which amplify the most the LOS path.*

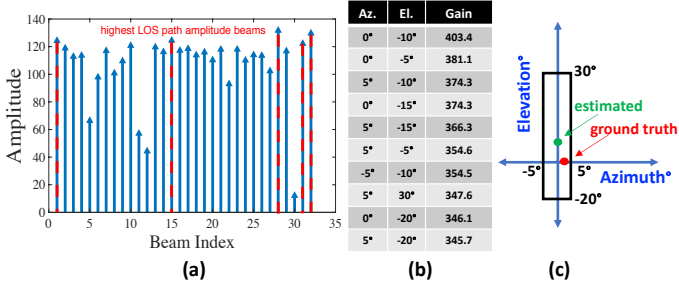


Figure 7: mWaveLoc angle identification example. (a) Beam refinement. (b) Gain computation and position ranking. (c) Position estimation.

To this end, *mWaveLoc* selects a constant number of M (out of the total N) beams that have the highest LOS path amplitude.³ Notice that, the selected M beams are not necessarily the highest SNR beams, since *mWaveLoc* ignores strong reflected paths. Then, *mWaveLoc* computes the overlap of these beams (*i.e.* the aggregate beam gain $G_a(\theta^{az}, \theta^{el})$ for each θ^{az}, θ^{el}). Since the degree of alignment of each beam with the LOS path may vary, *mWaveLoc* weights the contribution of each beam to $G_a(\theta^{az}, \theta^{el})$, based on its LOS path amplitude:

$$G_a(\theta^{az}, \theta^{el}) = \sum_{m \in M} \frac{A_m(\theta^{az}, \theta^{el})}{\max_{\forall m \in M, \forall \theta \in \Theta} \{A_m(\theta^{az}, \theta^{el})\}} \cdot \alpha_{los}^m \quad (2)$$

where $A_m(\theta^{az}, \theta^{el})$ is the gain (eq. 1) and α_{los}^m is the amplitude of LOS path, for beam m . The beam gains are normalized by the maximum gains across beams and directions.

Intuitively, the azimuth and elevation direction with the highest aggregate gain will be the direction of the LOS path. Hence, we could determine the position of the client as:

$$\hat{\theta}^{az}, \hat{\theta}^{el} = \operatorname{argmax}_{\theta^{az}, \theta^{el}} G_a(\theta^{az}, \theta^{el}) \quad (3)$$

However, our extensive experiments show that such an approach often performs poorly in 802.11ad commodity devices, due to their imperfect beam patterns. To this end, *mWaveLoc* adopts a *geometric* approach in device tracking. It first defines an area where a client can be located with high probability. Then, it selects the centroid of this area as client's angular position $\hat{\theta}^{az}, \hat{\theta}^{el}$. Specifically, *mWaveLoc* first ranks θ^{az}, θ^{el} directions based on their aggregate gain G_a (from the highest to the lowest). Then, it selects the set R of the highest gain (G_a) directions,⁴ and forms a rectangle, whose sides' lengths are $\max_{\theta^{az} \in R} \theta^{az} - \min_{\theta^{az} \in R} \theta^{az}$ and $\max_{\theta^{el} \in R} \theta^{el} - \min_{\theta^{el} \in R} \theta^{el}$. Finally, the center of the rectangle is an accurate estimation of client's angular position (as shown in Sec. 5).

Example: Figure 7 shows an example of *mWaveLoc*'s angular position identification with traces collected from our 802.11ad testbed. As shown in the figure, *mWaveLoc* first extracts the amplitude of

³Our extensive experiments show that setting M to 5 is sufficient for accurate estimation.

⁴Our offline training using extensive measurements shows that $|R| = 10$ maximizes *mWaveLoc* accuracy.

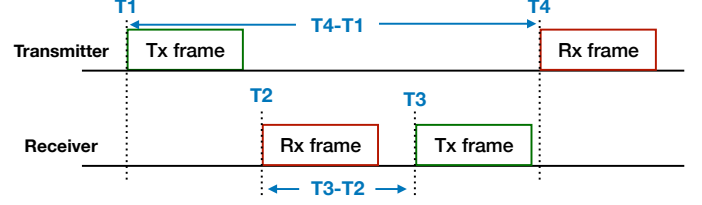


Figure 8: Timestamp estimation for ToF computation.

the LOS path for each beam and selects the M beams with the highest amplitude, annotated with dashed lines in Figure 7(a). Then, it computes the aggregated gain G_a for each position θ^{az}, θ^{el} , and ranks them as shown in Figure 7(b). Finally, it defines a rectangle with azimuth and elevation in the range of $[-5, 5]$ and $[-20, 30]$, respectively. The center of the rectangle (position estimated by *mWaveLoc*) is only 1.7° and 4.2° off in azimuth and elevation direction, from the ground truth position.

3.3 Tracking Distance

mWaveLoc leverages the IEEE 802.11 Fine Timing Measurement (FTM) scheme [30] implemented in our 802.11ad platform, to precisely measure the ToA (Time of Arrival) and ToD (Time of Departure) of frames exchanged between a transmitter and receiver pair. Upon appropriately calibrating such measurements, *mWaveLoc* estimates the ToF (Time of Flight), which is the round trip propagation time of a signal transmitted between an AP and a mobile device. Finally, it converts ToF to a transmitter-receiver separation distance.

FTM scheme has been widely used for Wi-Fi indoor localization [8, 18]. In such Wi-Fi systems ToF is read off the clock of the Wi-Fi radio when the signal arrives. Unfortunately, the clocks on today's Wi-Fi cards operate at tens of MHz, limiting their resolution in measuring time to tens of nanoseconds, causing the distance error in the order of meters. However, our 802.11ad platform employs a 21-tap fractional receiver filter (at 2.64*GHz), allowing for ~ 0.5 cm distance estimation granularity.

Figure 8 depicts the FTM 4-way handshake of our platform. Specifically, the transmitter (or initiator) requests to start fine timing measurement and observes the frames being sent by the receiver (or responder) device. The timestamps (T_1, T_4) and (T_2, T_3) are sampled by the digital modem of the transmitter and the receiver respectively, and they are reported by our 802.11ad firmware in picoseconds. Since transmitter and receiver use different clocks, T_1, T_4 and T_2, T_3 cannot be compared directly. To this end, *mWaveLoc* estimates ToF as:

$$ToF = (T_4 - T_1) - (T_3 - T_2) \quad (4)$$

Then, the transmitter-receiver distance (in meters) is:

$$Distance = \frac{ToF \cdot c}{2} \quad (5)$$

where c is the speed of light and ToF is expressed in seconds.

Calibration: The distance estimation based on equation 5 is still not accurate, since it does not take into consideration the propagation time of the signal from the sampling point (baseband) to the antenna edge. Specifically, as shown in Figure 9, the RF frontend of our platform is connected with the 802.11ad baseband, with a 46 cm long coaxial cable (for both transmitter and receiver sides).

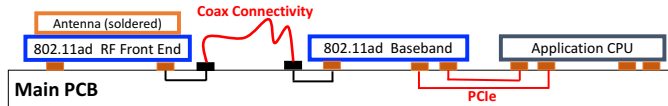


Figure 9: 802.11ad device architecture.

Algorithm 1 Channel Pruning and ToF Selection

```

1: Total beams:  $N$ , CIR tap:  $\tau$ 
2: Input: Measured channel  $\mathbf{h} : (h_1, \dots, h_N)$ 
3: Output: ToF timestamps  $T_1, T_2, T_3, T_4$ 
4: foreach  $h_i \in \mathbf{h}$ 
5:    $h'_i = \text{find\_peaks}(h_i)$  // CIR sanitization
6:   if  $h'_i(\tau_0) > h'_i(\tau_j) \forall \tau_j > \tau_0$  // LOS > NLOS path
7:      $H_i \leftarrow h'_i$ 
8:   endif
9: endfor
10:  $k' = \underset{k \in N}{\operatorname{argmax}}\{H_k(\tau_0)\}$ 
11:  $\{T_1, T_2, T_3, T_4\} \leftarrow \text{FTM}(k)$  // beam  $k$  for ToF collection

```

For ToF estimation, the cable length l_{coax} overheads add 4 times (one for each of the 4 frames of the handshake). Hence, for one way distance estimate, such overhead needs to be subtracted twice as follows:

$$\text{Dist} = \frac{\text{ToF} \cdot c}{2} - 2 \cdot l_{\text{coax}} \quad (6)$$

Note that, other circuit-related propagation delays such as propagation delay inside the RF module or from digital domain to DAC's output are negligible and are not taken into account in equation 6.

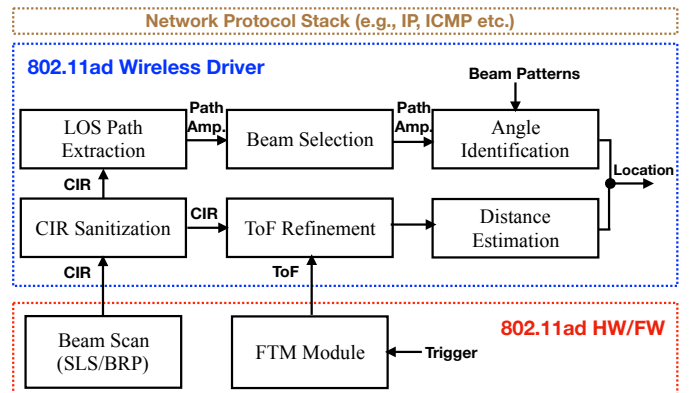
ToF-based distance estimation remains accurate even if there is channel contention from neighboring 802.11ad devices. Particularly, the time that a receiver waits to access the wireless medium is captured by T_2, T_3 timestamps (c.f. Fig. 8) and is ignored in the ToF estimation. We experimentally verify ToF's robustness to contention in Section 5.

3.4 Blockages and Multipath at 60 GHz

Multipath on ToF estimation: Because of indoor multipath environment, multiple copies (typically from 1 to 3) of the same signal arrive at the 60 GHz receiver. In settings of blockages or transmitter-receiver antenna misalignments, the reflected path(s) may be stronger than the LOS path, as shown in Figure 4(d). Since, the PHY layer reports the ToA timestamps of the strongest arriving signal path (which may not correspond to the LOS path), distance estimation may be erroneous for NLOS environments.

A CIR-based correction approach to addressing such multipath was proposed for Wi-Fi localization [8]. The key idea is that, the difference in delay between the strongest and first tap of the CIR could capture the positive bias in the ToA. However, the CIR-based correction depends on the CIR resolution. Our CIR resolution in 60 GHz is 0.57 ns (c.f. Sec. 3.2.1), causing a distance estimation error up to 17cm.

mWaveLoc leverages the channel measurements from multiple beams to improve ToF estimation accuracy. First, it identifies the beams where the reflected paths are stronger than the LOS path as shown in Figure 4(d), and then ignores ToF measurements from

Figure 10: Overview of *mWaveLoc*'s architecture at the Access Point side.

such beams. From the remaining beams, it uses the ToF measurements from the beam of the highest amplitude LOS path (first tap in the sanitized CIR). Note that our measurements show that in operational 60 GHz links, there is typically at least one beam whose LOS path is stronger than the reflected paths (c.f. Fig. 4). Hence, *mWaveLoc*'s ToF accuracy is not severely affected by multipath environments. This ToF sanitization process of *mWaveLoc* is illustrated in Algorithm 1 in greater detail.

Multipath on angular position estimation: *mWaveLoc* can identify the LOS path, regardless of the multipath environment, using CIR measurements. The beams that show very low amplitude LOS path will typically show very low SNR (based on our measurements), and they can be easily excluded from *mWaveLoc*'s angular position estimation.

Blockages: *mWaveLoc* can achieve accurate localization as soon as there is a LOS signal path component between AP and client devices. Such a LOS signal path component still exists when AP and client devices are blocked by an obstacle which can be penetrated by the 60 GHz signal (e.g. a plastic chair or a thin glass wall). However, impenetrable obstacles (such as humans) can result in localization errors of several meters, as we show in Section 5. Existing designs [21, 51] use inertial sensors to address such limitations. We are planning to extend *mWaveLoc* to address persistent blockages in our future work.

3.5 Putting Everything Together

Figure 10 shows an overview of *mWaveLoc*'s system architecture (at the AP side). Briefly, the beam scanning (SLS and BRP - c.f. Sec. 3.1) module, implemented in the firmware of our platform, scans available beams and collects CIR data for each beam. Note that, *mWaveLoc* does not need to explicitly trigger beam scanning, since SLS and BRP are triggered at fine-time scales by the beam alignment and PHY rate adaptation modules of our platform. Hence, *mWaveLoc* does not impose any additional overhead. SLS and BRP take 1.25 ms and 20 μ s, respectively in our platform.

Upon collecting CIR samples, *mWaveLoc* sanitizes them and extracts the LOS paths, as described in Section 3.2.1. Then, it only considers the M beams that amplify the most the LOS paths, and

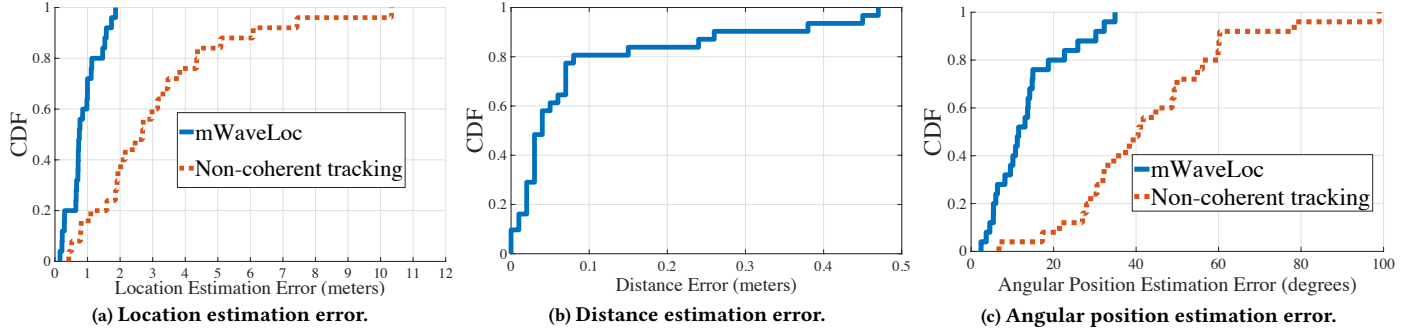


Figure 11: Localization error for *mWaveLoc* and non-coherent path tracking compared to ground truth, for multiple AP-client settings in the floorplan of Figure 12: (a) 3D location error, (b) distance estimation error, (c) angular position (azimuth, elevation) error.

uses their amplitudes along with the beam patterns to identify device’s angular position. In addition, *mWaveLoc* periodically triggers the FTM module in the firmware to collect ToF timestamps. Upon sanitizing them (*c.f.* Sec. 3.4), it finally computes the transmitter-receiver separation distance.

4 IMPLEMENTATION

We implemented *mWaveLoc* on our commercial off-the-shelf testbed shown in Figure 2, that includes AP and client devices, each equipped with a 4×8 element phased-array antenna which can generate beams in 3D space. AP’s and client’s 802.11ad chipsets are similar with the chipsets used by existing off-the-shelf 802.11ad devices [47]. Both devices support bit-rates up to 4.62 Gbps. Our AP platform runs an open-source OpenWrt [5] codebase on a dual-core 1.7 GHz CPU. Our client device runs Linux on a quad-core 2.2 GHz CPU. It can extract CIR measurements from the “Channel Estimation” (CE) header field of the IEEE 802.11ad data packets.

We have fully implemented *mWaveLoc* in the 802.11ad wireless driver (kernel-level) of our AP platform as shown in Figure 10. *mWaveLoc*’s kernel modules interact with the 802.11ad firmware functions using a highly efficient asynchronous wireless message passing interface. Specifically, the kernel issues “commands” to the firmware (such FTM or CIR collection trigger) and the firmware asynchronously responds to these commands providing the appropriate feedback (such as FTM timestamps and CIR measurements). *mWaveLoc* uses this feedback to accurately localize the client. Such feedback can be collected at millisecond scale in our platform. In the next section, we show that our system imposes almost zero overhead to 802.11ad throughput and our platform’s CPU utilization. Finally, *mWaveLoc* does not require any modifications to 802.11ad-compliant clients with FTM function support [30].

5 EVALUATION

In this section, we evaluate *mWaveLoc*’s location estimation accuracy by placing the AP and client devices in multiple locations in the enterprise floorplan of Figure 12. Our floorplan includes both rooms with concrete walls and an open area with cubicals of 1.2 meters height. We evaluate both static and mobile client settings, with both open LOS communication and blockages. *mWaveLoc* runs and estimates client’s 3D location at the AP.

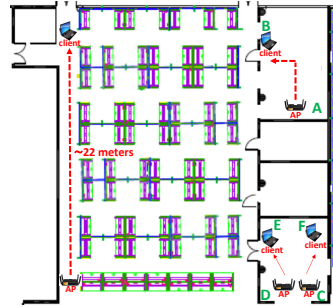


Figure 12: Experimental floorplan.

Ground truth: We consider as ground truth, the 3D location estimated using a HTC Vive base station and controller [52]. Vive’s tracking relies on infrared light emitted from the base station and received by 24 infrared sensors at the controller. Vive controller reports Cartesian coordinates which we convert to spherical (distance, azimuth, elevation) coordinates. Infrared-based positioning provides sub-millimeter accuracy in LOS settings, and has been widely used for VR applications [42]. Since Vive’s range is limited, we conduct most of our experiments with AP-client separation distance to be less than 7 meters. This is a common setting for dense 60 GHz AP deployments [55]. However, we still evaluate *mWaveLoc*’s location estimation accuracy in longer ranges ($> 20m$), using precise laser distance meters for ground truth.

Non-coherent tracking: We further compare *mWaveLoc* with non-coherent path tracking [14, 39], which does not require any special hardware and can be implemented in 802.11ad off-the-shelf devices (*c.f.* Sec. 2). Since such systems [14, 39] do not specify distance estimation algorithms, we use *mWaveLoc*’s distance estimation in our comparison.

5.1 Evaluation in Multiple Locations

We first evaluate *mWaveLoc*’s localization accuracy by placing our AP and client devices in multiple locations in the floorplan of Figure 12. We evaluate settings where AP and client separation distance varies from 0.25 to 22 meters. We evaluate a variety of elevation scenarios, by placing the AP and client from 1 to 2.6 meters height from the floor. In Figure 11a we first show the location estimation error distribution for *mWaveLoc* and non-coherent path tracking

algorithms. Here, error is defined as the euclidean distance of the estimated 3D-space (x, y, z) location compared to ground truth. We first observe that *mWaveLoc* achieves decimeter-level 3D localization accuracy (*i.e.* < 1 meter estimation error) in approximately 73% of the evaluated settings. Moreover, the median estimation error is 75 cm. On the other hand, the existing non-coherent path tracking approach can achieve decimeter-level location in only 17% of the evaluated settings. Non-coherent path tracking median and maximum estimation error is 2.7 and 10.3 meters, respectively.

We next investigate how much *mWaveLoc*'s angular position tracking (Sec. 3.2) and distance estimation (Sec. 3.3) modules contribute to 3D location estimation accuracy. To this end, in Figure 11b we first show *mWaveLoc*'s distance estimation error distribution over the ground truth AP-client separation distance. We observe that *mWaveLoc* achieves centimeter-level distance estimation accuracy in approximately 81% of the evaluated settings. Specifically, the median distance estimation error is 4 cm and it never exceeds 47 cm. Figure 11c further shows the angular position (azimuth, elevation) estimation error for *mWaveLoc* and non-coherent path tracking. The error is defined as the euclidean distance of the estimated position (θ^{az}, θ^{el}) compared to ground truth. We observe that *mWaveLoc*'s position error is less than 20° in 80% of the settings. The median position error for *mWaveLoc* is 11.5°, while for non-coherent path tracking is 40.5°. Next, we further investigate how the physical environment (*e.g.* moving obstacles), AP-client distance and mobility affect *mWaveLoc*'s performance.

5.2 Digging Deeper on *mWaveLoc*'s Performance

LOS settings: We first isolate the settings with perfect AP-client LOS communication and evaluate *mWaveLoc*'s performance. We consider that LOS will be the most common settings in very dense 60 GHz AP deployments [55] where devices support 360° coverage with multi-tile phase array antennas [15]. Note that in LOS settings there may be still reflectors which can create a strong multipath environment. We observe that *mWaveLoc* performs better in LOS than Non-LOS (NLOS) settings. Specifically, *mWaveLoc* achieves decimeter-level accuracy in 80% of the LOS settings (compared to 73% when we consider both LOS and NLOS settings). The highest localization error is 1.47 meters and it is observed in long range experiments, as we discuss next.

Interestingly, non-coherent path tracking still gives a median and maximum estimation error of 3.15 and 10.3 meters, respectively. Designs which simply correlate the beam patterns and their SNRs (such as non-coherent path tracking), could provide accurate position information only if the supported beams had very discrete spatial characteristics (*i.e.* highly directional beams). However, the imperfect beams (with strong side lobes) of commodity 802.11ad devices, and the use of SNR (instead of finer CIR feedback), lead to highly inaccurate estimation. We illustrate our point by investigating an example setting with perfect LOS, where AP-client separation distance is only 2.35 meters. We observe that, although 56.3% of the beams achieve similar, high SNR performance (between 33 dB and 34 dB), they may point to completely different directions. This is shown in the scatterplot of Figure 13 where x and y axis show the peak gain azimuth and elevation directions of the highest

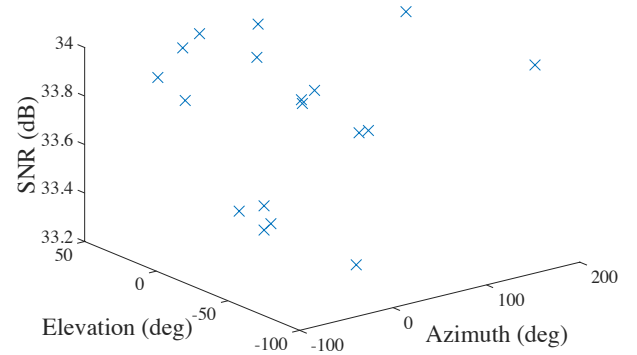


Figure 13: Azimuth and elevation directions that achieve the peak gains, for the highest SNR beams, of an example setting.

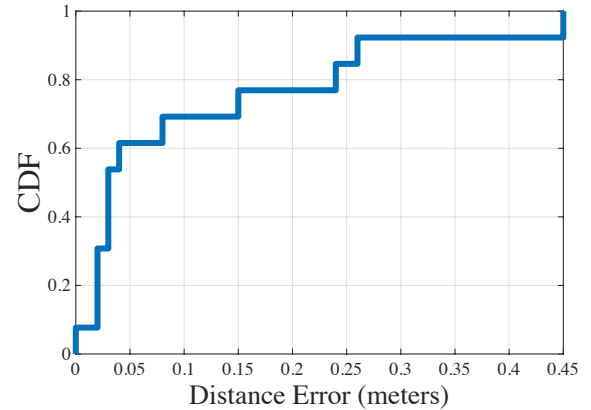


Figure 14: *mWaveLoc*'s distance estimation error in NLOS.

SNR beams, while z axis shows their SNR performance. Simply, correlating such SNRs and beam patterns results in a 1.9 meters localization error. *mWaveLoc* achieves 22 cm localization accuracy in the same setting.

NLOS settings: We next elaborate on NLOS settings, which include transient or permanent blockages of LOS communication and AP-client phased-array antennas' misalignment. Our results show that *mWaveLoc* achieves decimeter-level localization in the majority (60%) of the settings, with a median localization error of 73 cm. Figure 14 further shows that *mWaveLoc* can achieve centimeter-level distance estimation accuracy in approximately 70% of the NLOS evaluated settings (compared to 84% for the LOS settings). Decimeter localization accuracy can be achieved only if there is a LOS signal path component between AP and client devices. Our experiments show that, blockages such as leather chairs, thin glass walls, paper boxes, plastic blockages (*e.g.* trash cans) can be penetrated by 60 GHz signals allowing for accurate localization. However, *mWaveLoc*'s accuracy drops in the absence of a LOS path component as we discuss next.

Impenetrable blockages: Humans are typically impenetrable blockages for 60 GHz signals and can result in meter-level localization error. We create such scenario by having a person walking in-between a static AP and client placed 3.64 meters apart. Figure 15

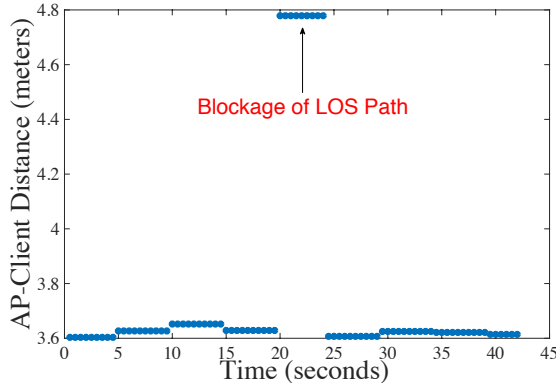


Figure 15: Impact of transient human blockages in *mWaveLoc*'s distance estimation accuracy.

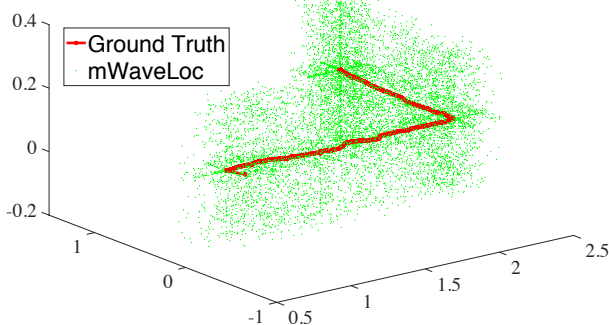


Figure 16: *mWaveLoc*'s localization performance in the pedestrian mobility setting shown in Figure 12.

shows the AP-client distance estimated by *mWaveLoc*, in time. We observe that although *mWaveLoc*'s estimated distance remains the same as the ground truth (3.64 meters) most of the time, when LOS is fully blocked by the human body, the estimated distance can go up to 4.78 meters (resulting in 1.14 meter error). Such severe blockages do not only affect localization accuracy but throughput performance as well. Specifically, human blockages can result in 70% TCP throughput drop. We are planning to extend *mWaveLoc* to address impenetrable blockages in our future work.

Coarse beam coverage and measurements: Interestingly, the highest localization errors observed in our experiments are not attributed to *mWaveLoc* system limitations, but to *beam coverage blind spots* and *coarse beam pattern measurements* provided by our 802.11ad chipset vendor. First, we observe that our platform's beam patterns may not adequately cover the entire 3D space. For example, at the setting we observed *mWaveLoc*'s highest localization error (of 1.86 meters), the client was placed at azimuth of 51.3° and elevation of 12.2°, where our AP's beams did not provide strong coverage. Second, the beam radiation patterns provided by our 802.11ad chipset vendor (*c.f.* Fig. 3) have been measured at a coarse 5° resolution. Such coarse resolution can introduce 10s of centimeters 3D localization error, even when the distance estimated by *mWaveLoc*'s FTM module is completely accurate.

Mobility: *mWaveLoc* can track a client's position at very fine time granularity (*millisecond* scale) and can accommodate fast mobility

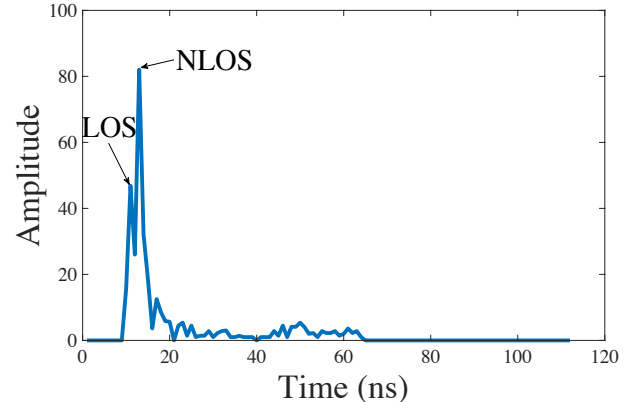


Figure 17: Multipath environment in a LOS setting where AP-client separation distance is 22 meters.

scenarios, as we further discuss in the following section. We have verified *mWaveLoc*'s robustness to mobility in multiple scenarios, such as the one illustrated in Figure 12, where a mobile client is moving from position *A* to *B* at pedestrian speed. Figure 16 shows the ground truth (measured by our HTC devices) and *mWaveLoc*'s position estimation. We observe that *mWaveLoc* can accurately track client's 3D position with a median estimation error of 17 cm. The maximum location estimation error is 36 cm.

Ground truth distance (m.)	Location error (cm) max/min/median	Distance error (cm) max/min/median
(0, 4)	76.7/21.5/29.4 cm	6/0/1 cm
[4, 6)	113/71.5/99.7 cm	7/3/4 cm
[6, 22]	146.5/71.1/84.9 cm	47/7/38 cm

Table 1: *mWaveLoc*'s 3D localization accuracy and distance estimation accuracy as a function of AP-client separation distance.

Impact of AP-client separation distance: Next, we investigate the impact of AP-client separation distance in *mWaveLoc*'s localization performance. We isolate the impact of distance by excluding the NLOS settings (as defined above) from our study. Table 1 shows *mWaveLoc*'s 3D location estimation error and AP-client distance estimation error for settings where AP-client distances vary from 0.25 to 22 meters. When the distance is between 0 to 4 meters, *mWaveLoc*'s location estimation error is 29.4 centimeters in the median case. However, when we increase the separation distance, the localization error increases as shown in the last two rows of Table 1. This increase is mainly attributed to the higher *mWaveLoc*'s distance estimation error, which can go up to 47 cm, as shown in the last column of Table 1. Interestingly, we observe that, such distance estimation error is not attributed to 802.11ad FTM limitations to provide accurate timestamps over long distances. Our results show that as the signal propagation path increases, the probability of higher multipath due to strong reflectors increases, resulting in stronger NLOS than LOS paths. For example, when we placed an AP and client devices 22 meters apart (in perfect LOS) as shown in Figure 12, we observed that typically the NLOS path's amplitude was higher than the LOS. This is shown in the Power Delay Profile of Figure 17 for the highest CIR beam. Although *mWaveLoc*'s ToF

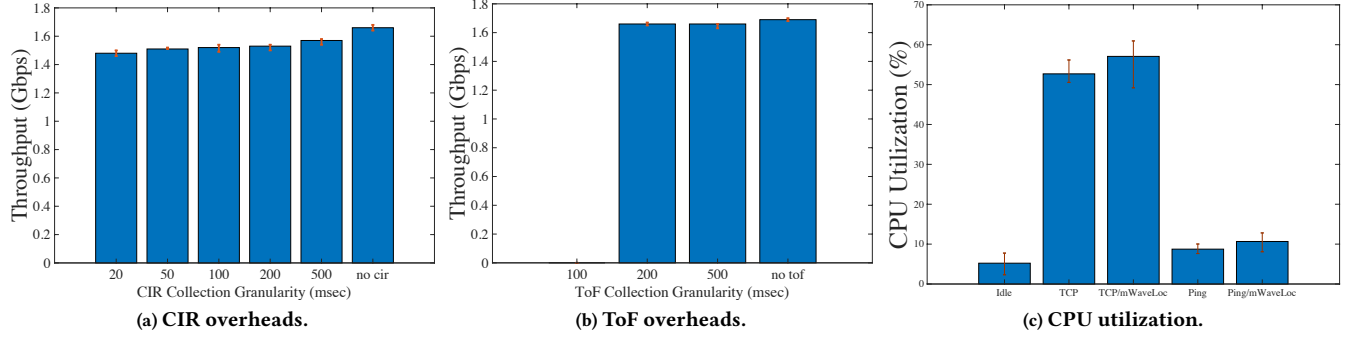


Figure 18: *mWaveLoc* system overheads: (a) CIR collection impact on TCP throughput performance, (b) ToF collection impact on TCP throughput performance, (c) *mWaveLoc* CPU utilization (%) aggregated over both cores at the AP side, for three different traffic scenarios.

sanitization module is robust to multipath, there can be still distance errors, when ToF is estimated based on the NLOS path. Apart from the distance error, the angular error enlarges the location error when the distance between the AP and client increases.

Channel contention: Interfering traffic from neighboring 802.11ad devices does not affect *mWaveLoc*'s localization accuracy, as discussed in Section 3.3. We have experimentally verified *mWaveLoc*'s robustness to contention, by setting up two contending pair of nodes (*C, D, E, F*), as shown in Figure 12. In our experiment, the two APs being approximately 1 meter apart, are sharing the 60 GHz channel. Our results show that *mWaveLoc*'s location estimation accuracy, remains the same if either or both pairs are active at the same time.

5.3 *mWaveLoc* System Latency and Overheads

An important goal for *mWaveLoc* localization is to be able to track a client's position at very fine time granularity (*millisecond* scale). This is a key requirement for high mobility scenarios (e.g. vehicle localization). Different from existing localization designs (e.g. [37, 50]) which require multiple APs coordinated by a controller, *mWaveLoc* can achieve this latency requirement by fully running at a single AP. Then, CIR collection at the AP through SLS and BRP takes only 1.25 ms and 20 μ s respectively in our platform (c.f. Sec. 3.5). Moreover, ToF timestamp collection is in the order of μ s, since FTM frames can be sent at Gbps PHY rates.

Implementation overheads in our platform: *mWaveLoc* runs in the kernel of our AP platform and interacts with the firmware and hardware through a message passing interface (c.f. Sec 4). This interaction adds a small overhead in CIR and ToF collection as we describe next.

We first evaluate the impact of fine-grained CIR collection on TCP throughput performance. We generate saturated TCP traffic from the AP to client, and we evaluate the TCP throughput performance degradation, when collecting CIR samples at increasing granularities. Figure 18a shows that, when collection granularity is 20ms, the throughput performance degradation is 10.8%.⁵ When we decrease the collection granularity to 200ms and 500ms the throughput degradation becomes 7.8% and 5.4% respectively. The

collection overhead is negligible for higher CIR collection granularities. Moreover, when traffic is not saturated, even 20 ms CIR collection granularity does not affect TCP throughput performance.

Figure 18b further shows how ToF timestamp collection affects TCP throughput. First, due to our platform's implementation limitations, ToF collection cannot be triggered at the kernel level, at time granularities less than 150ms. However, for ToF collection granularities greater than 150ms, we observe that the throughput degradation is negligible. For example, for 200ms collection frequency, the TCP throughput degradation is only 1.8%.

Finally, we evaluate the additional CPU overhead of running *mWaveLoc* in our AP platform. Specifically, we measure the CPU utilization aggregated over both CPU cores for three traffic settings; (a) no traffic (i.e. idle), (b) saturated TCP traffic, and (c) low-rate ping traffic, with and without *mWaveLoc*. In our experiments, *mWaveLoc* collects ToF timestamps at the finest (150ms) time granularity. Figure 18c shows that on average *mWaveLoc* increases the CPU utilization by only 4.4% and 1.9% for TCP and ping traffic, respectively. In conclusion, *mWaveLoc* can support high mobility scenarios with negligible overhead, in off-the-shelf 802.11ad platforms.

6 CONCLUSION

In this paper, we have designed and implemented *mWaveLoc*, the key building block of 3D localization for 802.11ad 60 GHz mmWave networks. *mWaveLoc*'s goals are *high-accuracy* and *practicality*. In terms of accuracy, *mWaveLoc* seeks to achieve decimeter-level 3D localization that can enable a wide range of new applications (e.g. position dependent VR/AR). Next, *mWaveLoc* is designed to be highly practical; *single-AP*, *robust* (to mobility and blockages), *802.11-compliant*, no client support, and *lightweight* localization. *mWaveLoc* judiciously leverages the *directional* and *short-wavelength* properties of 802.11ad 60 GHz networks for highly accurate 3D localization. Our real-life prototype and experiments with off-the-shelf 802.11ad testbeds show that *mWaveLoc* can indeed achieve decimeter-level 3D localization accuracy in realistic indoor scenarios, where a LOS path exists between AP and client devices. We believe *mWaveLoc* will serve as a key building block for 3D localization in the next-generation 5G networks.

⁵The errorbars indicate the min and max throughput values.

REFERENCES

- [1] 2015. FCC Promotes Higher Frequency Spectrum for Future Wireless Technology. <https://apps.fcc.gov>.
- [2] 2015. Verizon applauds FCC chairman's move to 5G spectrum. goo.gl/OvNyzZ.
- [3] 2016. Unlocking the Promise of Broadband for All Americans. goo.gl/XzCvVv.
- [4] Microsoft. X-box Kinect. <http://xbox.com>
- [5] OpenWrt. Wireless Freedom. <https://openwrt.org/>
- [6] Omid Abari, Haitham Hassanieh, Michael Rodriguez, and Dina Katabi. 2016. Millimeter Wave Communications: From Point-to-Point Links to Agile Network Connections. In *ACM HotNets-XV'16*.
- [7] Alain Olivier, Guillermo Bielsa, Irene Tejado, Michele Zorzi, Joerg Widmer, Paolo Casari. 2016. Lightweight Indoor Localization for 60-GHz Millimeter Wave Systems. In *IEEE SECON'16*.
- [8] Alex T. Mariakakis, Souvik Sen, Jeongkeun Lee, Kyu-Han Kim. 2014. SAIL: Single Access Point-based Indoor Localization. In *ACM MobiSys'14*.
- [9] Arash Shahmansoori, Gabriel E. Garcia, Giuseppe Destino, Gonzalo Seco-Granados, Henk Wymeersch. 2015. 5G Position and Orientation Estimation through Millimeter Wave MIMO. In *IEEE Globecom Workshops*.
- [10] Aruba Networks, Inc. 2017. Location Services Platform. <http://www.arubanetworks.com>.
- [11] Chi Zhang, Xinyu Zhang. 2017. Pulsar: Towards Ubiquitous Visible Light Localization. In *ACM MobiCom'17*.
- [12] Christopher R. Anderson, Theodore S. Rappaport. 2004. In-Building Wideband Partition Loss Measurements at 2.5 and 60 GHz. *IEEE Transactions on Wireless Communications* 3, 3.
- [13] Cisco Systems, Inc. 2016. HyperLocation: Best Practices and Troubleshooting Guide. <https://www.cisco.com> (2016).
- [14] Daniel Steinmetzer, Daniel Wegemer, Matthias Schulz, Joerg Widmer, Matthias Hollick. 2017. Compressive Millimeter-Wave Sector Selection in Off-the-Shelf IEEE 802.11ad Devices. In *ACM CoNEXT'17*.
- [15] Debabani Choudhury, Richard Roberts, Ulun Karacaoglu. 2017. Wireless Antenna Array System Architecture and Methods to Achieve 3D Beam Coverage. *USA Patent US959576B2* (2017).
- [16] Deepak Vasish, Swaran Kumar, Dina Katabi. 2016. Decimeter-Level Localization with a Single WiFi Access Point. In *USENIX NSDI'16*.
- [17] Dimitrios Lymberopoulos, Jie Liu, Xue Yang, Romit Roy Choudhury, Vlado Handziski, Souvik Sen. 2015. A Realistic Evaluation and Comparison of Indoor Location Technologies: Experiences and Lessons Learned. In *ACM IPSN'15*.
- [18] Domenico Giustiniano, Stefan Mangold. 2011. CAESAR: Carrier Sense-based Ranging in Off-the-shelf 802.11 Wireless LAN. In *ACM CoNEXT'11*.
- [19] Dongyao Chen, Kang G. Shin, Yurong Jiang, Kyu-Han Kim. 2017. Locating and Tracking BLE Beacons with Smartphones. In *ACM CoNEXT'17*.
- [20] Facebook, Inc. 2016. Introducing Facebook's new terrestrial connectivity systems — Terragraph and Project ARIES. <https://code.facebook.com/posts/1072680049445290/introducing-facebook-s-new-terrestrial-connectivity-systems-terrapherad-and-project-aries/>.
- [21] G. Oberholzer, P. Sommer, R. Wattenhofer. 2011. SpiderBat: Augmenting wireless sensor networks with distance and angle information. In *ACM/IEEE IPSN'11*.
- [22] Georg Gerstweiler, Emanuel Vonach, Hannes Kaufmann. 2016. HyMoTrack: A Mobile AR Navigation System for Complex Indoor Environments. *Sensors* 16, 1 (2016).
- [23] Gu, Yanying and Lo, A. and Niemegeers, I. 2009. A Survey of Indoor Positioning Systems for Wireless Personal Networks. *Commun. Surveys Tuts.* (2009).
- [24] Guillermo Bielsa and Joan Palacios and Adrian Loch and Daniel Steinmetzer and Paolo Casari and Joerg Widmer. 2018. Indoor Localization Using Commercial Off-The-Shelf 60 GHz Access Points. In *IEEE INFOCOM'18*.
- [25] R. C. Hansen. 2009. *Phased Array Antennas*. John Wiley & Sons, Inc.
- [26] Hao Zhang, Chunlei Wu, Xuerong Cui, T. Aaron Gulliver, Hongqiao Zhang. 2013. Low complexity AOA based codebook beamforming for 60 GHz wireless communications. In *IEEE PACRIM'13*.
- [27] Carlo Fischione Hazemi El-Sayed, George Athanasiou. 2014. Evaluation of Localization Methods in Millimeter-Wave Wireless Systems. In *IEEE CAMAD'14*.
- [28] Hua Deng, Akbar M. Sayeed. 2014. Mm-wave MIMO channel modeling and user localization using sparse beamspace signatures. In *IEEE SPAWC'14*.
- [29] IEEE Standards Association. 2012. IEEE Standard 802.11ad-2012, Amendment 3: Enhancements for Very High Throughput in the 60 GHz Band. goo.gl/r2JeYd.
- [30] IEEE Standards Association. 2016. Part 11: Wireless LAN Medium Access Control (MAC) and Physical Layer (PHY) Specifications.
- [31] Jiali Zhang, Xinyu Zhang, Pushkar Kulkarni, Parameswaran Ramanathan. 2016. OpenMili: A 60 GHz Software Radio Platform with a Reconfigurable Phased-Array Antenna. In *ACM MobiCom'16*.
- [32] Joan Palacios, Paolo Casari, Joerg Widmer. 2017. JADE: Zero-Knowledge Device Localization and Environment Mapping for Millimeter Wave Systems. In *IEEE INFOCOM'17*.
- [33] Joe Chen and Daniel Steinmetzer and Jiska Classen and Edward W. Knightly and Matthias Hollick. 2017. Pseudo Lateration: Millimeter-Wave Localization Using a Single RF Chain. In *IEEE WCNC'17*.
- [34] Joydeep Biswas, Manuela Veloso. 2012. Depth Camera Based Indoor Mobile Robot Localization and Navigation. In *IEEE ICRA'12*.
- [35] Junyi Wang and Zhou Lan and Chin-Sean Sun and Chang-Woo Pyo and Jing Gao and Tuncer Baykas and Azizur Rahman and Ryuhei Funada and Fumihide Kojima and Ismail Lakkis and Hiroshi Harada and Shuzo Kato. 2009. Beamforming Codebook Design and Performance Evaluation for 60GHz Wideband WPANs. In *IEEE VTC'09*.
- [36] Kejriwal, Surabhi and Mahajan, Saurabh. 2015. Smart Buildings: How IoT Technology Aims to Add Value for Real Estate Companies. *Deloitte University Press* (2015).
- [37] Manikanta Kotaru and Sachin Katti. 2017. Position Tracking for Virtual Reality Using Commodity WiFi. In *CVPR'17*.
- [38] Manikanta Kotaru, Kiran Joshi, Dinesh Bharadia, Sachin Katti. 2015. SpotFi: Decimeter Level Localization Using WiFi. In *ACM SIGCOMM'15*.
- [39] Yanzi Zhu Upamanyu Madhow Haitao Zheng Maryam Esfandi Rasekh, Zhinus Marzi. 2017. Noncoherent mmWave Path Tracking. In *ACM HotMobile'17*.
- [40] Theodore S. Rappaport, Felix Gutierrez, Eshar Ben-Dor, James N. Murdoch, Yijun Qiao, and Jonathan I. Tamir. 2013. Broadband Millimeter-Wave Propagation Measurements and Models Using Adaptive-Beam Antennas for Outdoor Urban Cellular Communications. *IEEE Transactions on Antennas and Propagation* 61, 4 (2013).
- [41] Theodore S. Rappaport, Robert W. Heath Jr., Robert C. Daniels, and James N. Murdoch. 2014. *Millimeter Wave Wireless Communications*. Prentice Hall.
- [42] Oculus Rift. 2018. <https://www.oculus.com/>. (2018).
- [43] Sangki Yun, Yi-Chao Chen, Huizhuang Zheng, Lili Qiu, Wenguang Mao. 2017. Strata: Fine-Grained Acoustic-based Device-Free Tracking. In *ACM MobiSys'17*.
- [44] Sanjib Sur, Ioannis Pefkianakis, Xinyu Zhang, Kyu-Han Kim. 2017. WiFi-Assisted 60 GHz Wireless Networks. In *ACM MobiCom'17*.
- [45] Sanjib Sur, Vignesh Venkateswaran, Xinyu Zhang, Parmesh Ramanathan. 2015. 60 GHz Indoor Networking through Flexible Beams: A Link-Level Profiling. In *ACM SIGMETRICS'15*.
- [46] Ralph O. Schmidt. 1986. Multiple Emitter Location and Signal Parameter Estimation. *IEEE Transactions on Antennas and Propagation* 34, 3 (1986).
- [47] Keith Shaw. 2016. Acer TravelMate 802.11ad notebook: An industry 'first' you might never need or use. www.networkworld.com/
- [48] Peter F. M. Smulders. 2009. Statistical Characterization of 60-GHz Indoor Radio Channels. *IEEE Transactions on Antennas and Propagation* 57, 10 (2009).
- [49] Song Liu, Tian He. 2017. SmartLight: Light-weight 3D Indoor Localization Using a Single LED Lamp. In *ACM SenSys'17*.
- [50] Souvik Sen, Dongho Kim, Stephane Laroche, Kyu-Han Kim, Jeongkeun Lee. 2015. Bringing CUPID Indoor Positioning System to Practice. In *WWW'15*.
- [51] Souvik Sen, Jeongkeun Lee, Kyu-Han Kim, Paul Congdon. 2013. Avoiding Multi-path to Revive Inbuilding WiFi Localization. In *ACM MobiSys'13*.
- [52] Vive VR System. 2018. <https://www.vive.com/us/product/vive-virtual-reality-system/>. (2018).
- [53] Teng Wei, Anfu Zhou, Xinyu Zhang. 2017. Facilitating Robust 60 GHz Network Deployment By Sensing Ambient Reflectors. In *USENIX NSDI'17*.
- [54] Teng Wei, Xinyu Zhang. 2015. mTrack: High-Precision Passive Tracking Using Millimeter Wave Radios. In *ACM MobiCom'15*.
- [55] Teng Wei, Xinyu Zhang. 2017. Pose Information Assisted 60 GHz Networks: Towards Seamless Coverage and Mobility Support. In *ACM MobiCom'17*.
- [56] Edward W. Knightly Joerg Widmer Thomas Nitsche, Adriana B. Flores. 2015. Steering with Eyes Closed: mm-Wave Beam Steering without In-Band Measurement. In *IEEE INFOCOM'15*.
- [57] Xuerong Cui, Thomas A. Gulliver, Juan Li. 2016. Vehicle Positioning Using 5G Millimeter-Wave Systems. *IEEE Access'16* (2016).
- [58] Zulkuf Genc, Bao Linh Dang, Jing Wang, Ignas Niemegeers. 2008. Home Networking at 60 GHz: Challenges and Research Issues. *Springer Annals of Telecommunications* 63 (2008), 501–509.